CLEAN
Soil Air Water

Mohammad Hossein Sowlat[1,2,3]
Kazem Naddafi[1,2]
Masud Yunesian[1,2]
Peter L. Jackson[4]
Saeedeh Lotfi[5]
Abbas Shahsavani[1]

[1]Department of Environmental Health Engineering, School of Public Health, Tehran University of Medical Sciences, Tehran, Iran
[2]Institute for Environmental Research (IER), Tehran University of Medical Sciences, Tehran, Iran
[3]Students' Scientific Research Center (SSRC), Tehran University of Medical Sciences, Tehran, Iran
[4]Environmental Science and Engineering, University of Northern British Columbia, Prince George, Canada
[5]Department of Environment and Energy, Science and Research Branch, Islamic Azad University, Tehran, Iran

Research Article

PM_{10} Source Apportionment in Ahvaz, Iran, Using Positive Matrix Factorization

Source apportionment of particulate matter <10 μm in diameter (PM_{10}), having considerable impacts on human health and the environment, is of high priority in air quality management. The present study, therefore, aimed at identifying the potential sources of PM_{10} in an arid area of Ahvaz located in southwest of Iran. For this purpose, we collected 24-h PM_{10} samples by a high volume air sampler. The samples were then analyzed for their elemental (Al, As, B, Ba, Be, Ca, Cd, Co, Cr, Cu, Fe, Hg, K, Mg, Mn, Na, Ni, Pb, Se, Si, Sn, Sr, Li, Ti, V, Zn, Mo, and Sb) and ionic (NH_4^+, Cl^-, NO_3^-, and SO_4^{2-}) components using inductively coupled plasma optical emission spectrometry and ion chromatography instruments, respectively. Eight factors were identified by positive matrix factorization: crustal dust (41.5%), road dust (5.5%), motor vehicles (11.5%), marine aerosol (8.0%), secondary aerosol (9.5%), metallurgical plants (6.0%), petrochemical industries and fossil fuel combustion (13.0%), and vegetative burning (5.0%). Result of this study suggested that the natural sources contribute most to PM_{10} particles in the area, followed closely by the anthropogenic sources.

Keywords: Elemental composition; Ionic components; PM10; Positive Matrix Factorization; Source apportionment

Received: March 14, 2012; *revised:* September 14, 2012; *accepted:* September 21, 2012

DOI: 10.1002/clen.201200131

1 Introduction

Sources of particulate matter are broadly categorized as natural (such as wind-blown dust, marine aerosol, forest fires, volcanic ash, etc.) and anthropogenic (such as industries, motor vehicles, biomass burning, fossil fuel combustion, etc.). While the former has had a constant role in global air pollution, the latter has become an increasing concern due to the rapid pace of urbanization and industrialization during the past century [1]. Particulate matter with aerodynamic diameter <10 μm (PM_{10}) plays a distinct role in air pollution, mainly because of its noticeable respiratory and cardiovascular health effects [2], and that it can be the potential carrier of harmful heavy metals such as As, Cd, Pb, and Zn [3]. Environmental impacts, such as changes in the radiation budget of the earth, the atmosphere's thermal structure, and the troposphere's chemical composition, have also been associated with enhanced levels of PM_{10} [4–6]. Some authors believe that these impacts depend mainly on the geographic location [7] and the composition of the potential sources in that area [8], making it necessary to fully identify the sources to explore the possible mechanisms of the mentioned impacts and to be capable of efficiently managing and mitigating the air pollution [9].

Positive matrix factorization (PMF) is a receptor model which has been recently used for identifying the sources of air pollutants that can be chemically or physically speciated and analyzed [10]. The advantages of PMF over other statistical multivariate methods, such as principal component analysis (PCA) which were previously in use for this purpose, are improved capability to properly handle uncertainties, ability to deal with noisy data sets, and no need for detailed prior knowledge of the existing sources in the area [11–13]. In the past decade, therefore, PMF has been used to identify the potential sources of different size ranges of particulate matter in different areas of the world [8, 9, 11, 14, 15].

In the latest report of the World Health Organization (www.who.int/phe) [16], Ahvaz, located in an arid area in southwest of Iran, was identified as the most polluted city in the world regarding atmospheric PM_{10} pollution. This is thought to be mainly due to the occurrence of the Middle Eastern dust (MED) storms, caused primarily by the Shamal wind carrying large amounts of dust particles from Iraqi deserts to the area [16–18]. As a consequence, daily mean PM_{10} concentrations of up to 5012.7 $\mu g/m^3$ have been recorded in the area [19]. The main objective of the present study was, therefore, to identify the potential sources of PM_{10} and their relative contributions to the total mass of PM_{10} in Ahvaz by using the PMF receptor model. For this purpose, PM_{10} data were collected over the period from April 2010 through March 2011, and were then chemically analyzed for their elemental composition, including Al, As, B, Ba, Be, Ca, Cd, Co, Cr, Cu, Fe, Hg, K, Mg, Mn, Na, Ni, Pb, Se, Si, Sn, Sr, Li, Ti, V, Zn, Mo, and Sb, and ionic components, including NH_4^+, Cl^-, NO_3^-, and SO_4^{2-}. We also applied conditional probability function (CPF) and some elemental ratios in order to further explore the validity of the outputs of the PMF model.

Correspondence: Dr. K. Naddafi, Department of Environmental Health Engineering, School of Public Health, Tehran University of Medical Sciences, Enghelab St., Tehran, Iran
E-mail: kazem.naddafi@gmail.com

Abbreviations: CPF, conditional probability function; **ICP-OES**, inductively coupled plasma optical emission spectrometry; **MDL**, method detection limit; **PCA**, principal component analysis; **PM_{10}**, particulate matter with aerodynamic diameter <10 mm; **PMF**, positive matrix factorization; **S/N**, signal to noise

2 Material and methods

2.1 Sampling

Ahvaz, the most polluted city of the world with respect to atmospheric PM_{10} pollution, is the capital of Khuzestan Province, Iran, with a total population of 1.3 million. It is an arid area located in a highly gas- and oil-rich region in southwestern Iran (a latitude of 31°20′N and a longitude of 48°40′E). Therefore, a variety of oil-related industries, such as oil extraction and refining as well as petrochemistry, exist in the area. In addition, low vegetation cover, highly humid weather (with a maximum seasonal average of 57% in summer), considerably high air temperatures (with a maximum seasonal average of 37°C in summer), and strong surface winds are the main characteristics of the area. This, in combination with close proximity to southern Iraqi deserts (the leading origin of mineral dusts in the region [16]) have caused severe dust storms that highly deteriorate the air quality in the study area [18, 19]. Motor vehicles and seasonal vegetative burning (mostly reed beds) are known to be other types of air pollutant sources in the area. Figure 1 illustrates the location of the study area with respect to the nearby sources.

The sampling was systematically carried out every six days over the period from April 2010 to March 2011. PM_{10} samples were collected on 20 cm × 25 cm glass-fiber filters by using a high volume air sampler (Model: Anderson). The sampler was installed at a height of 10 m above the ground on the roof top of the Health Research Center and operated at a flow rate of 1 m^3/min. The installation height of 10 m was selected because it minimizes the undesirable effects of local traffic emissions as well as both natural and anthropogenic obstacles on the air trajectory, which can in turn affect the PM_{10} concentrations [11].

Before the sampling, the filters were washed with distilled-deionized water to remove impurities, and were then put into an oven operating at 50°C for 10 h [20]. Afterwards, the filters were kept at constant temperature (20 ± 1°C) and relative humidity (40 ± 5%) for 24 h before being weighed by an analytical balance (Model: Sartorius 2004 MP) which had a reading precision of 10 μg. After the sampling, the filters were again kept at constant temperature and relative humidity (20 ± 1°C and 40 ± 5%) before being weighed for the second time. Finally, after calculating the PM_{10} concentrations by the above-mentioned gravimetric method, the filters were kept in plastic bags in a refrigerator at 4°C until they were chemically analyzed [21–23].

2.2 Chemical analysis of water-soluble ions and trace elements

One-fourth of each filter paper was used to determine the concentrations of four water-soluble ions, namely, NH_4^+, Cl^-, NO_3^-, and SO_4^{2-}, in PM_{10}. This part of the filter paper was cut and shredded before being put into a 100 mL vial containing 50 mL of distilled-deionized water which had a resistivity of 18 MΩ cm. To extract the ionic components from the filter paper, the vial was shaken for 2 h. After being filtered through a membrane which had a pore size of 0.2 μm (Schleicher & Schuell), the extracts were poured into a plastic vial and kept at 4°C [24, 25]. We then used an ion chromatography (Model: Metrohm 850 Professional IC, Switzerland) to obtain the concentrations of the ionic components in PM_{10}. The flow rate of the instrument was adjusted at 0.7 mL/min. The cationic solvent contained nitric acid 3.2 mM, while the anionic solvent consisted of a combination of sodium bicarbonate 1.7 mM and sodium carbonate 1.8 mM. The injection rate of the cationic solvent (10 μL) differed from that of the anionic solvent (20 μL). The recovery rates ranged 80–120% for the ionic components.

To obtain the concentrations of the trace elements (including crustal elements and heavy metals), another one-fourth of each filter paper was digested by an acid mixture, consisting of 3 mL HNO_3, 1 mL HCl, and 1 mL HF, at 170°C for 4 h. The digestion process was done in a Teflon digestion vessel since high pressures were applied. Having cooled and dried the extracts, they were diluted to 10 mL of distilled-deionized water which had a resistivity of 18 MΩ cm [26]. Finally, we applied an inductively coupled plasma optical emission spectrometry (ICP-OES) to determine the concentrations of 28 elemental components of PM_{10}, including Al, As, B, Ba, Be, Ca, Cd, Co, Cr, Cu, Fe, Hg, K, Mg, Mn, Na, Ni, Pb, Se, Si, Sn, Sr, Li, Ti, V, Zn, Mo, and Sb.

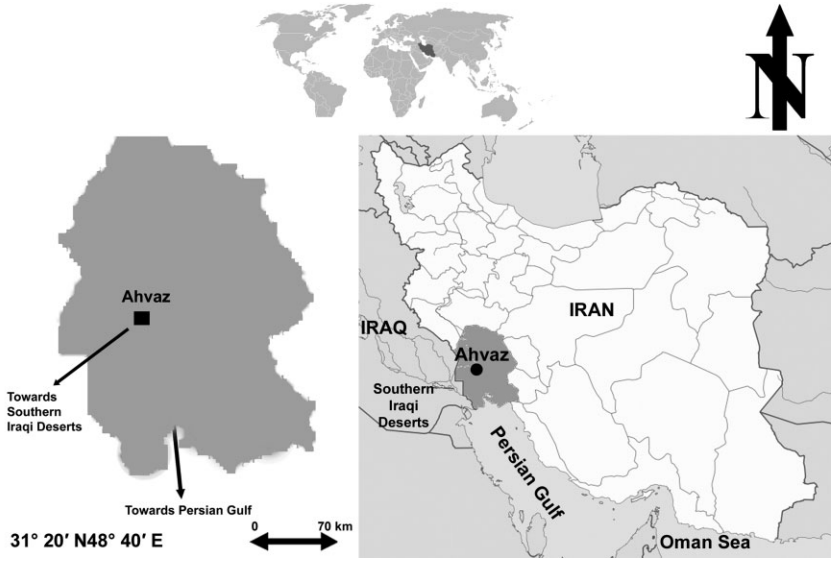

Figure 1. Location of the sampling station with respect to the nearby sources.

2.3 Positive matrix factorization (PMF)

PMF is a receptor model based on multivariate statistical methods and was first introduced by Paatero and Tapper [27]. PMF is based on the decomposition of a large, chemically or physically speciated data set into two smaller matrices, i.e., factor profiles and factor contributions. At the next step, an expert should interpret the matrices to infer source types taking into account the resolved source profiles, and with the aid of wind rose analysis as well as emission inventories [10].

PMF uses the weighted least-squares fits for a dataset. The weights in the matrix (data set) can be modified by the expert in accordance with the experimental uncertainties, including uncertainties occurring during the sampling and those due to the analytical errors, for each entry in the data set. Although it is allowed in PCA, in PMF none of the factors can have negative contributions to any of the sources. The main objective of PMF model is to identify a number of potential sources (p), the profile of species in each source (f), and the relative contributions of all of the sources to each of the collected samples, according to the following equation [28, 29]:

$$x_{ij} = \sum_{k=1}^{p} g_{ik} f_{kj} + e_{ij} \tag{1}$$

where x_{ij} is the matrix x containing i samples and j species; g_{ik} is the relative contribution of kth factor to the jth samples; f_{kj} is the relative contribution of jth species to the kth factor; and e_{ij} is the residual concentration of the jth species in the ith samples which is not resolved by PMF.

Taking into account the uncertainties in the data set, a solution minimizing the weighted sum of the squared residual function (Q) is provided by PMF according to the following equation [28, 29]:

$$Q = \sum_{i=1}^{n} \sum_{j=1}^{m} \left[\frac{x_{ij} - \sum_{k=1}^{p} g_{ik} f_{kj}}{u_{ij}} \right]^2 \tag{2}$$

where u_{ij} is the uncertainty associated with the concentration of x_{ij}.

It is noteworthy that the USEPA PMF software (version 3.0) was used in the present study.

2.4 Data handling

In this work, to estimate the background concentration of each species over the study area, we chemically analyzed unexposed blank filters in a regular basis during the study period. According to the guideline proposed by previous studies [30], the method detection limit (MDL) for each species was calculated by adding three standard deviations to the mean values of the chemically analyzed unexposed blank filters.

We used box plates to explore the existence of outlier data (both very high and very low concentrations) for each species. Then we selected the concentrations as high as three times of the inter-quartile range [11] for illustration on the time-series graph. These outlier data were discarded from the data set unless they followed the general temporal trend of the concentrations for that species.

According to the guideline proposed by Polissar et al. [31], we replaced the missing values (mainly those discarded from the dataset) by the geometric mean of that species. This was done primarily to maintain a sufficient number of samples required for modeling. It is mentioned by some authors that this action can artificially change the correlations which exist among the species. To handle this and to decrease the weight of these values on the model outputs, an uncertainty of four times as high as the geometric mean was set for each [8, 11]. Finally, to handle the values below the MDL for each species, they were replaced by half of the MDL for that species, and their uncertainties were set as 5/6 of the MDL [31].

The PMF model input uncertainties mainly encompass sampling (due either to the sampling device or to the operator) and analytical (likewise, due either to the analytical instruments or to the laboratory operator) errors. All of the mentioned types of the uncertainties are usually reported by the analytical laboratory or the agency in charge of reporting the data [10].

In case the species concentration is above the MDL, the following equation is applicable for calculating the uncertainty [10]:

$$\text{Unc} = \sqrt{(\text{error fraction} \times \text{concentration})^2 + (\text{MDL})^2} \tag{3}$$

2.5 Conditional probability function (CPF)

Meteorological data can be applied to help identify the possible locations of the nearby sources. For this purpose, we used CPF that was first introduced by Ashbaugh et al. [32]. A combination of source contributions and meteorological data (wind speed and direction) is used in CPF, and the final value is calculated by the following equation:

$$\text{CPF} = \frac{m_{\Delta\theta}}{n_{\Delta\theta}} \tag{4}$$

where $m_{\Delta\theta}$ shows the number of occurrences from the wind sector $\Delta\theta$ that are higher than the threshold criterion (that was set as the 25th percentile); and $n_{\Delta\theta}$ is representative of the total number of occurrences from that wind sector ($\Delta\theta$) overall. Our wind direction data were divided into 16 sectors, so we set the $\Delta\theta$ at 22.5°. Hours during which the wind speed was $<1\ \text{m s}^{-1}$ were excluded from CPF calculations. CPF can have values ranging from 0 to 1, with higher values indicating the likely location of nearby point sources. It should be noted that according to the study of Kim et al. [33], in order to match the daily average collected samples to hourly wind direction and wind speed data, each hour of the day was assumed to have the same source contribution as that of the day as a whole.

3 Results

Over the entire study period, 72 24-h PM_{10} samples were collected in the study area. Table 1 presents some of the most important parameters for the PMF input data such as missing values, values below the MDL, and S/N (signal to noise) ratio. S/N ratio is a statistical variable indicating if the variability of the measured concentrations is real or it is due to the variability in the noise of the data. This ratio is calculated by the following equation [10]:

$$\frac{\text{S}}{\text{N}_\text{j}} = \sqrt{\frac{\sum_{i=1}^{n} (x_{ij} - s_{ij})^2}{\sum_{i=1}^{n} s_{ij}^2}} \tag{5}$$

S/N ratio is directly affected by the percent of missing values and values below the MDL for each species. If the values of these

CLEAN Soil Air Water

Table 1. Summary statistics for critical parameters of PMF speciated input data

Species	Missing values (out of 72 samples)	MDL ($\mu g/m^3$)	Values below the MDL (out of 72 samples)	S/N ratio
PM_{10}	0	–	0	98.73
Al	2	0.3	0	48.49
As[a)]	5	0.06	1	22.67
B	12	5	11	8.72
Ba	0	0.1	1	29.33
Be	1	0.01	1	23.64
Ca	1	5	0	20.10
Cd[a)]	2	0.065	0	47.92
Co[a)]	0	0.01	0	32.17
Cr[a)]	0	0.15	0	45.78
Cu[a)]	0	0.011	0	32.33
Fe	7	1.615	17	9.34
Hg[a)]	0	0.26	0	41.24
K	6	3	0	7.44
Mg	3	1	0	16.23
Mn[a)]	0	0.39	3	42.73
Na	0	0.252	0	89.23
Ni[a)]	16	0.99	28	4.95
P	2	0.01	0	35.78
Pb[a)]	0	0.01	0	33.48
Se[a)]	0	0.05	0	29.09
Si	0	0.051	0	32.33
Sn[a)]	1	0.014	0	31.25
Sr[a)]	0	0.02	0	32.28
Li	13	0.025	5	6.12
Ti[a)]	0	0.08	0	45.15
V[a)]	0	0.1	0	36.73
Zn[a)]	0	0.15	0	38.80
Mo[a)]	9	0.1	27	7.93
Sb	0	0.0105	0	21.71
NH_4^+	0	0.0001	15	32.33
Cl^-	13	0.00005	30	9.00
NO_3^-	10	0.00005	21	10.11
SO_4^{2-}	8	0.00005	12	11.50

[a)] The MDL of the elements market by the asterisk are shown in ng/m^3.

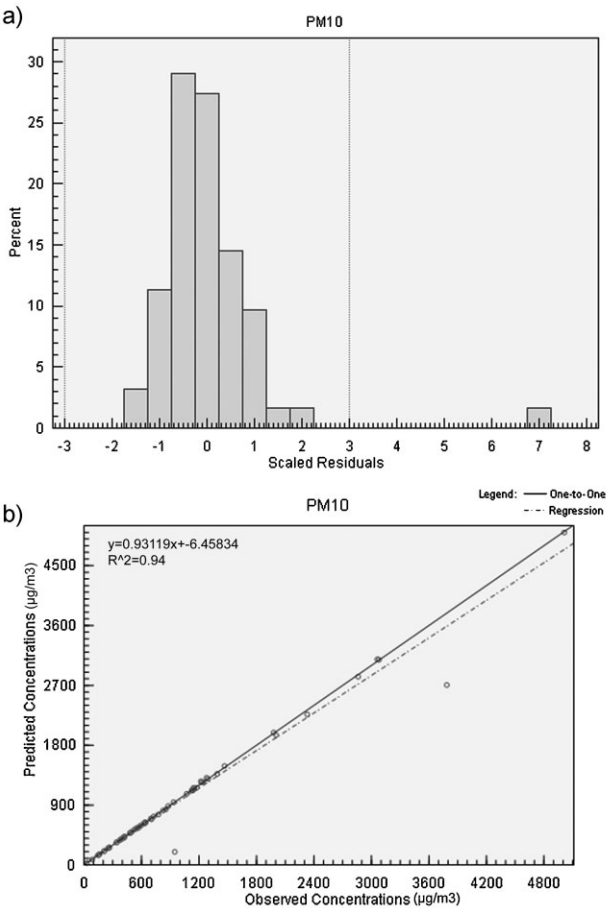

Figure 2. Residual analysis (a) and regression line between measured and predicted concentrations of PM_{10} (b).

parameters are high for a species, it means lack of variability in the measurements. As a result, that species cannot meaningfully contribute to source identification. For this reason, the PMF model automatically reduces the weight of such species in the calculations [10]. As given in Tab. 1, most of the species in our data set had quite high S/N ratios. However, for some species, like B, Fe, K, Ni, Li, Zn, and Cl^-, the ratio was lower than those of others, due mainly to high percentage of either missing values or values below the MDL or both; nonetheless, they were still higher than the desired S/N ratio of 2 [12].

The PMF model was run several times with different Fpeak values, extra model uncertainties, and number of factors. After a thorough evaluation and interpretation of each model run, the eight-factor solution, with an extra model uncertainty of 15% and an Fpeak value of 0.1, was found to be the most physically probable solution.

The residual analysis of the model run for PM_{10} data is shown in Fig. 2a. The nearly normal shape of the histogram indicates the fitness of the model to the input data. Figure 2a also indicates some underestimations that have been made by the model, which is possibly due to the presence of considerably high PM_{10} concentrations during dust storms (e.g., the maximum PM_{10} concentration of 5012.68 $\mu g/m^3$) compared to such low values as the minimum concentration of 28.27 $\mu g/m^3$ during non-dust, clean days. Figure 2b illustrates the correlation between predicted and observed values of PM_{10}. These values are generally well correlated with each other ($R^2 = 0.94$), showing that the PM_{10} data were reasonably modeled by PMF. The effect of overestimations can also be observed in the regression line.

Mean relative contributions of each of the resolved factors for the PM_{10} data are depicted in Fig. 3. It can be observed that 41.5% of the overall mass concentration of PM_{10} was attributed to factor 1 which is attributed to crustal dust, while other factors had relative contributions in the range of 5–13%. Figure 4a and b illustrates the species profile for each of the factors resolved by PMF. The marker species used to identify each source are marked by darker color.

Figure 5 shows the time-series curves for the temporal variations of factors 1 and 3, while the seasonal as well as day-of-the-week box plots for factors 1–3 are illustrated in Fig. 6a–d. These graphs are not shown for other factors because no distinct trends were observed for them. Finally, Fig. 7 depicts the conditional probably function calculated for each factor during the study period. Figures 5–7 have been used as critical aids in interpreting the factors resolved by the PMF model.

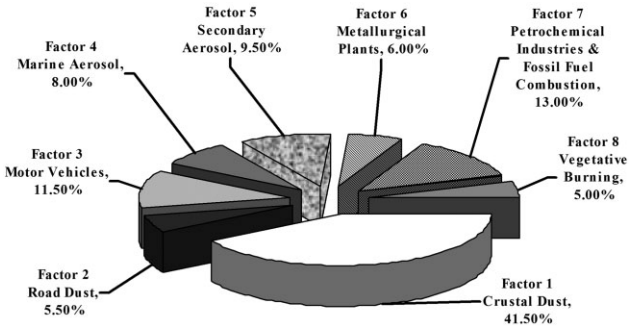

Figure 3. Mean relative contributions of the eight factors resolved by PMF.

4 Discussion

4.1 Factor identification

4.1.1 Factor 1

The first factor, having the highest contribution (41.5%), was found to be ''crustal dust'' since it is prevailed by well-known crustal soil markers such as Al (52.6%), Ca (45.5%), Fe (23%), Si (47.8%), K (9.0%), Mg (6.4%), and Mn (32.5%) [9, 11, 14]. This can be further supported by the temporal trend of this factor, which indicates significantly higher values during spring and summer in comparison with those observed during fall and winter (Figs. 5 and 6a). It was found by the previous studies that dust storms most frequently happen during the same time period [18, 19]. During some days in spring and summer, such as May 26, 2010, the relative contribution of this factor sharply increased up to 80%. These days temporally matched the dust storm days with significantly high PM_{10} concentrations during the study period (in the case of May 26, the maximum

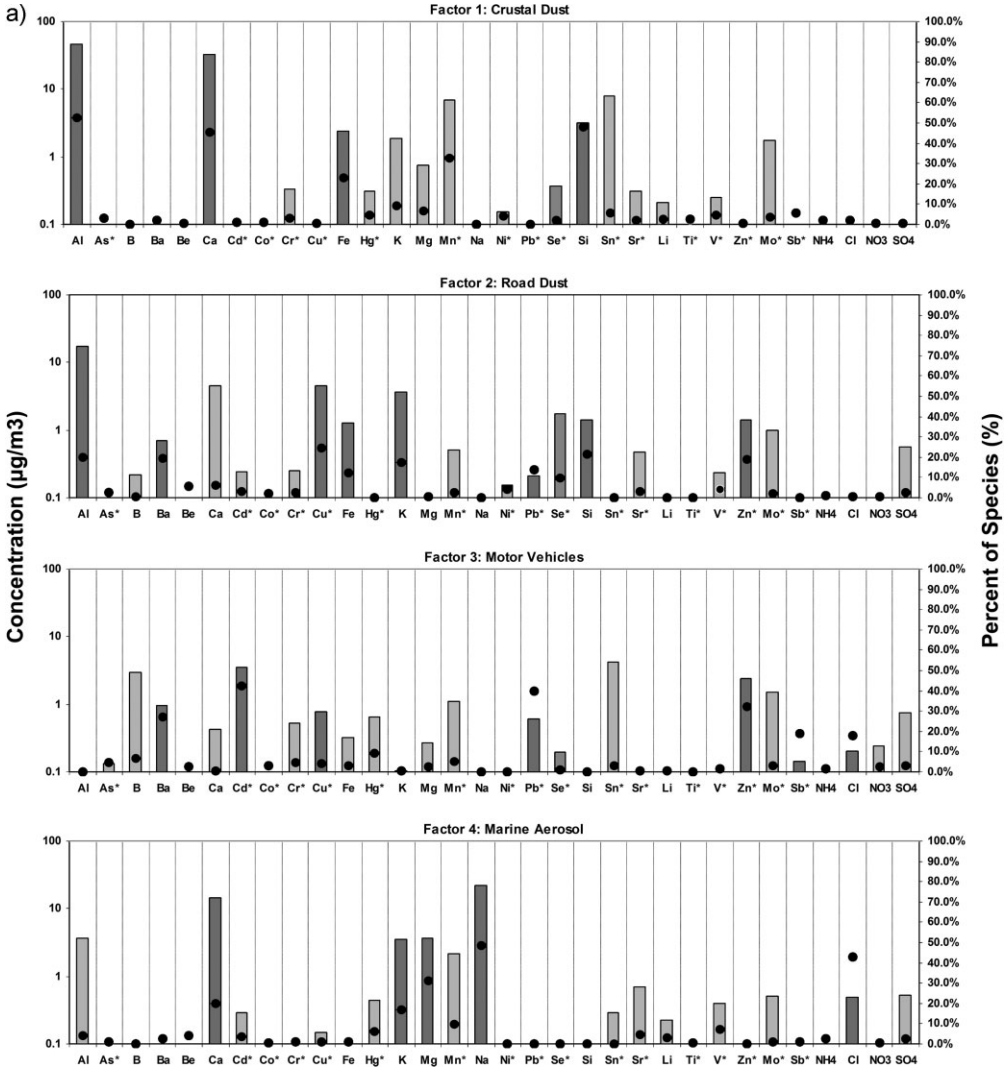

Figure 4. Species profiles of each factor resolved by PMF; (a) factors 1–4; (b) factors 5–8 (solid circles are representative of the relative contribution of each species in percent; bar diagrams indicate the relative contributions in $\mu g/m^3$; the relative contributions of the species marked by asterisk are presented in ng/m^3).

CLEAN Soil Air Water

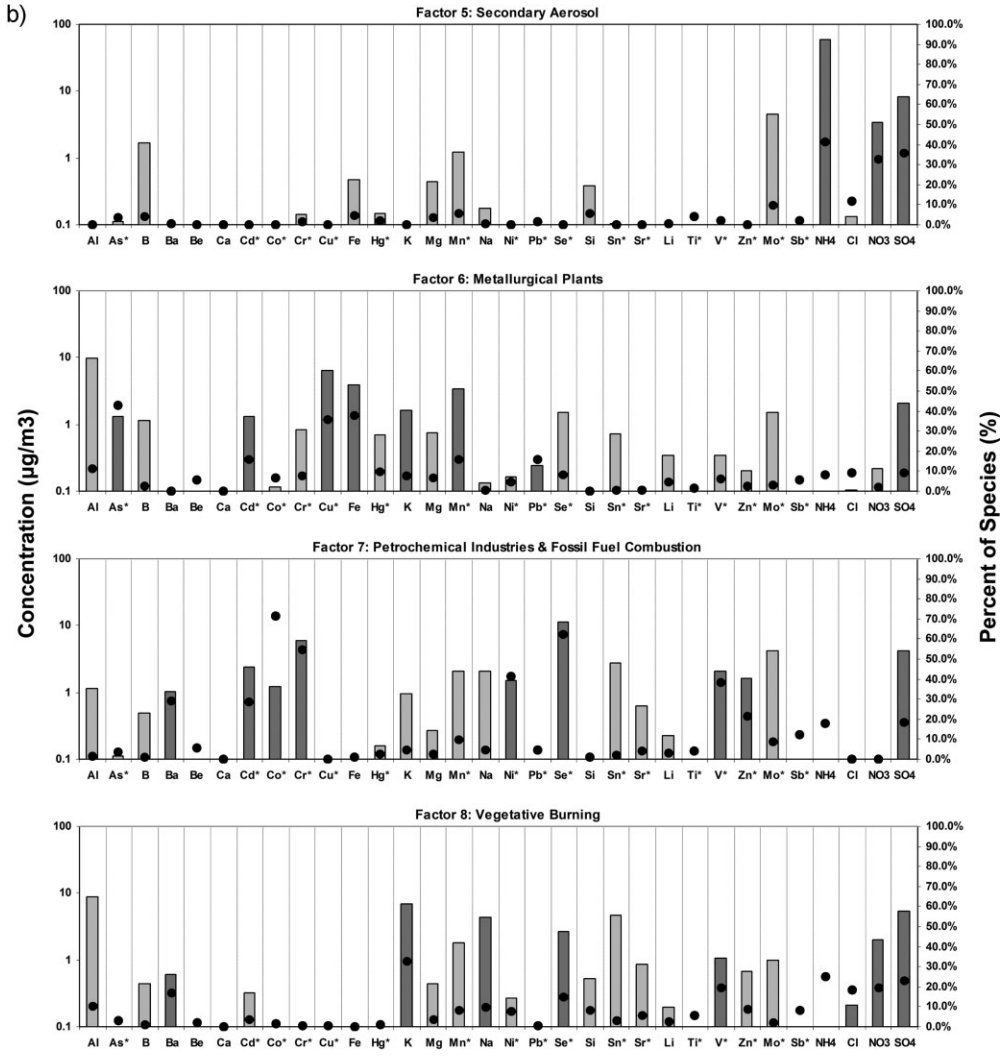

Figure 4. (*Continued*)

concentration of 5012.68 $\mu g/m^3$ was observed). In addition, the CPF graph (Fig. 7) indicates that this factor mainly originates from western and southwestern areas. This is also in agreement with our interpretation, because it was reported by the previously conducted studies in the area that the occurrence of dust storms is most likely during spring and summer due primarily to the Shamal wind which blows from west and transports huge amounts of dust particles from Iraqi deserts to the study area [16, 17].

4.1.2 Factor 2

The second factor contributes to only 5.5% of the total mass of PM_{10}. It is believed that this factor best suits the ''road dust'' source category since it is dominated by a variety of crustal elements, such as Al (19.7%), Fe (12.1%), K (17.2%), and Si (21.2%), and a number of anthropogenic elements, including Ba (19.4%), Cu (24.6%), Pb (13.6%), Se (9.7%), and Zn (18.9%) [34]. According to Lim et al. [9], this source category originates primarily from the transportation of motor vehicles in paved and non-paved roads. As a result, a combination of road dust deposited on the roads and vehicular emissions (including exhaust emissions and abrasion of tires) can be released from this source category [35]. This interpretation can be validated by the day-of-the-week box plot presented for this factor (Fig. 6d). It is shown in the figure that this factor has higher contributions during weekdays compared to weekends. CPF calculations indicated no distinct wind sector for this factor, although there was a slightly higher frequency with southwesterly winds. Lack of a distinct wind pattern can also imply the impact of motor vehicles on this factor, as with the third factor (motor vehicles).

4.1.3 Factor 3

The third factor is mainly dominated by Ba (26.8%), Cd (42.5%), Cu (4.3%), Pb (39.6%), Zn (32%), Sb (18.8%), and Cl^- (17.8%), which are known as the tracers of ''motor vehicles'' source category [9, 36, 37]. Motor vehicles contributed to 11.5% of the total mass of PM_{10}. In contrast with crustal dust category, higher relative contributions were observed for this factor in fall and winter compared to spring and summer (Figs. 5 and 6b). This could be attributed to the fact that the transformation of exhaust emissions into solid particles is highly

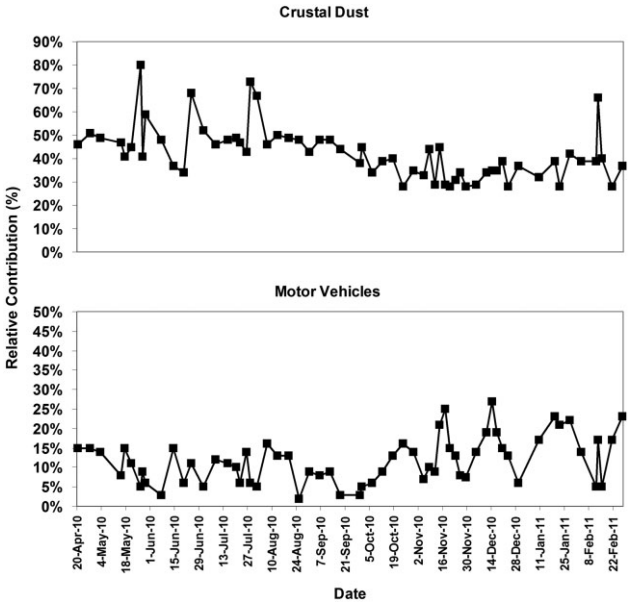

Figure 5. Temporal trends of relative contributions of crustal dust and motor vehicles to the total mass of PM_{10}.

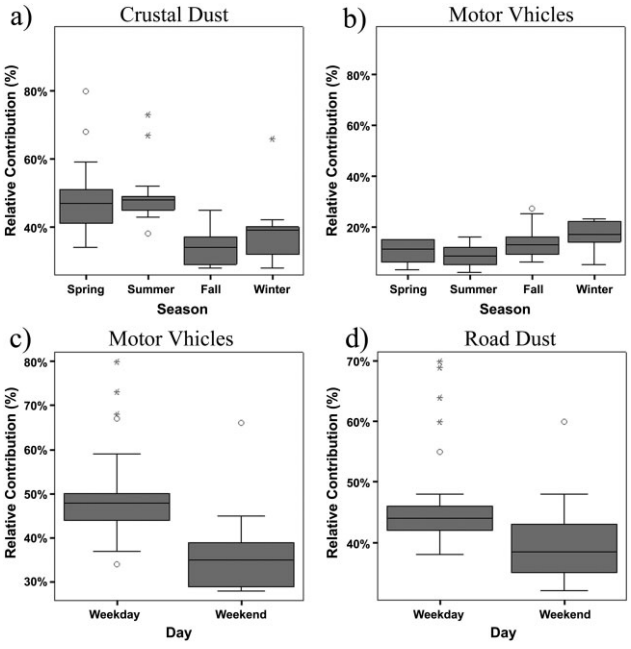

Figure 6. Seasonal (a and b) and day-of-the-week (c and d) box plots for the relative contribution of factors 1–3 (the box represents the upper and lower quartiles; the horizontal line in the box is the median of the date; whiskers indicate the minimum and maximum values excluding the outliers; circles represent the outliers; and asterisks are the extreme values).

facilitated in low atmospheric temperatures [38]. In addition, atmospheric stability and the following thermal inversions can intensify the effect of vehicular emissions during fall and winter. The day-of-the-week box plot, indicating higher contributions of this factor in weekdays than those observed in weekends, further supports the hypothesis that this factor is mainly affected by motor vehicles. According to CPF calculations (Fig. 7), there was no highly distinct

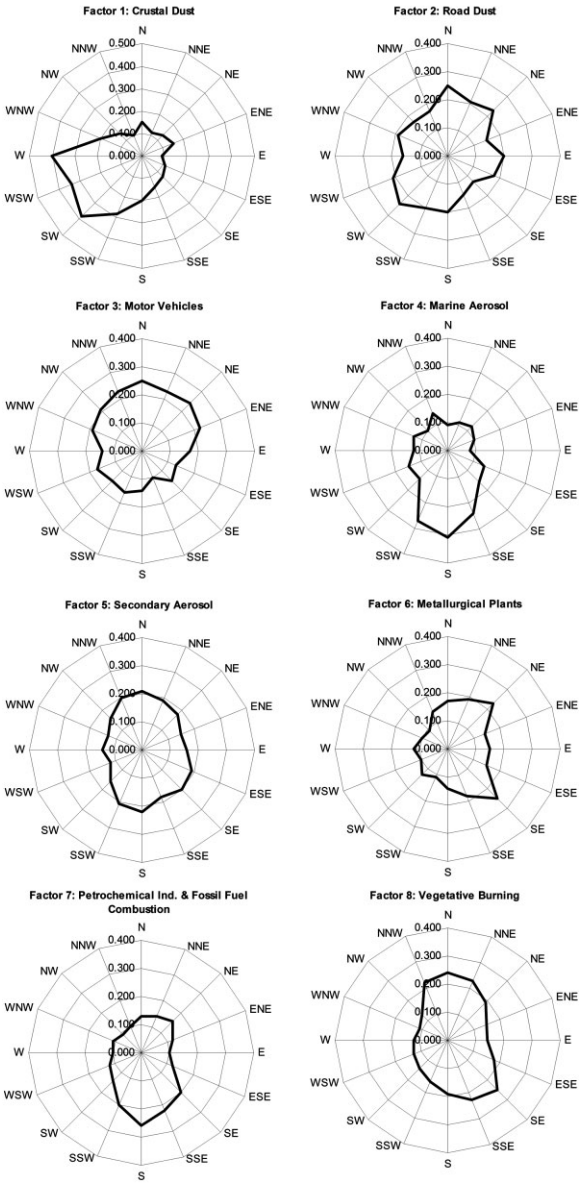

Figure 7. CPF for the factors resolved by PMF.

wind sector for this factor since vehicular emission are not released from a limited number of large sources; rather, vehicular emissions are generated by a large number of small sources well distributed across the city. However, it should be noted that since the sampling site was located in the southern part of the city, greater CPF values were observed for northerly wind sectors.

4.1.4 Factor 4

The fourth factor, which accounted for 8% of the total mass of PM_{10}, is primarily prevailed by Na (48.7%) and Cl^- (43%), which are knows as the most important tracers of ''marine aerosol'' [37, 39] to marine aerosol source category [11]. This can be further supported by a Na/Mg ratio of 7.2, which was introduced as a good indicator of marine aerosol [40]. The CPF graph for this factor (Fig. 7) clearly reflects higher relative contributions when the wind came from the

south. Since the Persian Gulf is located south of the city (Fig. 1), marine aerosol is the most likely source category.

4.1.5 Factor 5

The fifth factor contributed to 9.5% of the total mass of PM_{10}. This factor most possibly suits ''secondary aerosol'' source category since it is dominated by NH^{4+} (41.3%), NO_3^- (32.4%), and SO_4^{2-} (35.8%), which are believed to be tracers of secondary nitrate and sulfate aerosols [14, 37, 39]. Precursors of secondary nitrate aerosols mainly originate from industrial activities and motor vehicles [41]. Secondary sulfate aerosols originate from photochemical processes at high temperatures and relative humidity in summer [42], and from combustion of fossil fuels at highly stable atmospheric conditions in winter [43]. The CPF graph for this factor (Fig. 7) indicated no distinct wind pattern. This is primarily because secondary aerosols result from the transformations of primary air pollutants, which are emitted directly into the atmosphere; hence, finding the exact location of the possible sources is quite difficult. However, the slight inclination of this graph towards northern and southern wind sectors implies the impact of motor vehicles and industrial activities, respectively.

4.1.6 Factor 6

A variety of metallic elements, including As (42.9%), Cd (15.6%), Cu (35.6%), Fe (37.8%), K (7.8%), Mn (15.6%), and Pb (15.7%), and a number of ionic components, such as NH_4^+ (8.2%), Cl^- (9.2%), and SO_4^{2-} (9.1%), dominated this factor; therefore, it best suits ''metallurgical plants'' source category according to previously conducted studies [9, 11, 14, 37]. Metallurgical plants contributed to 6% of the total mass of PM_{10}. The CPF graph for this factor (Fig. 7) indicates higher contributions during northeasterly and southeasterly winds.

4.1.7 Factor 7

The seventh factor, accounting for 13% of the total mass of PM_{10}, encompasses Ba (29%), Cd (28.5%), Co (71.4%), Cr (54.8%), Ni (39.8%), Se (14.8%), V (19.5%), Zn (21.5%), NH_4^+ (17.9%), and SO_4^{2-} (18.4%). These species have been introduced as good markers of ''petrochemical industries'' and ''combustion of fossil fuels'' [11, 37, 44]. Another useful indicator used for identifying this source category is the Ni/Zn ratio. The ratio of 2.2 observed here is in agreement with that observed by Allamen et al. [11] (2.34). CPF calculations (Fig. 7) indicated that the relative contributions were higher during the southerly winds, where petrochemical industries are mainly located.

4.1.8 Factor 8

The eighth factor belongs mainly to Ba (17%), K (32.4%), Na (9.8%), Se (6.2%), V (38.5%), NH_4^+ (25%), Cl^- (18.3%), NO_3^- (19.5%), and SO_4^{2-} (23%). Al, Si, and K have been linked to the ''combustion of biomass or vegetation'' [14, 39]. Na, NH_4^+, Cl^-, and SO_4^{2-} have also been known as good tracers of vegetative burning by other studies [9]. Therefore, this factor seems to best suit the ''vegetative burning'' source category. The presence of this factor was expected due mainly to the seasonal burning of reed beds near the study area. The CPF graph (Fig. 7) suggests that these reed beds are most likely located south of the city. Finally, it is noteworthy that since some industrial complexes were located in the vicinity of these reed beds and fields, some of the elements that are commonly linked to the industry (such as Ba, V, and Se), which are not specific markers of vegetative burning, have also been considered by the model as the markers of this source.

4.2 Number of factors

Even though some mathematical criteria have been suggested for choosing the optimum number of factors, most of the studies have based this on minimization of the *Q* values as well as interpretation of the resolved source profiles according to the approximate knowledge of existing sources in the study area [31]. In the present study, the same method was applied. Therefore, the model was run with different number of factors, i.e., between 4 and 10, and the effects of the changes were evaluated. Fpeak values were also systematically changed in order to obtain low and relatively constant *Q* values [45]. Finally, we have also taken into account the value of extra model uncertainties, which is representative of uncertainties other than those occurring during sampling or chemical analysis in the laboratory [10]. As mentioned earlier, eight factors, with an Fpeak value of 0.1 and an extra model uncertainty of 10%, was found to be the most physically reasonable solution for the dataset.

5 Conclusions

The present study was conducted with the aim of identifying the possible sources of PM_{10} in an arid area in southwestern Iran by using the PMF receptor model. For this purpose, we used a large data set consisting of 32 species (28 elements and 4 ions). According to the results of the PMF model, eight factors were resolved: crustal dust (41.5%), road dust (5.5%), motor vehicles (11.5%), marine aerosol (8.0%), secondary aerosol (9.5%), metallurgical plants (6.0%), petrochemical industries and fossil fuel combustion (13.0%), and vegetative burning (5.0%). It was found that almost half of the total mass of PM_{10} in the area originates from natural sources, while the other half is released from anthropogenic sources. High contribution of natural sources was most probably due to the occurrence of dust storms in the area. These findings can be considered by policy-makers to effectively design air pollution mitigation and management schemes.

Acknowledgments

The present study was funded by Tehran University of Medical Sciences (research grant number #9742) and Institute for Environmental Research (IER).

The authors have declared no conflict of interest.

References

[1] K. Naddafi, M. H. Sowlat, M. H. Safari, Integrated Assessment of Air Pollution in Tehran, over the Period from September 2008 to September 2009, *Iran. J. Public Health* **2012**, *4*, 77.

[2] C. A. I. Pope, D. W. Dockery, J. Schwartz, Review of Epidemiological Evidence of Health Effects of Particulate Air Pollution, *Inhal. Toxicol.* **1995**, *7*, 1.

[3] D. W. Dockery, C. A. Pope III, Acute Respiratory Effects of Particulate Air Pollution, *Annu. Rev. Public Health* **1994**, *15*, 107.

[4] F. Dentener, G. Carmichael, Y. Zhang, J. Lelieveld, P. Crutzen, Role of Mineral Aerosol as a Reactive Surface in the Global Troposphere, *J. Geophys. Res.* **1996**, *101*, 869.

[5] H. Liao, Y. L. Yung, J. H. Seinfeld, Effect of Aerosols on Tropospheric Photolysis Rates in Clear and Cloudy Atmospheres, *J. Geophys. Res.* **1999**, *104*, 23697.

[6] S. K. Satheesh, K. Krishna Moorthy, Radiative Effects of Natural Aerosols: A Review, *Atmos. Environ.* **2005**, *39*, 2089.

[7] F. Dominici, A. McDermott, M. Daniels, S. L. Zeger, J. M. Samet, Revised Analyses of the National Morbidity, Mortality, and Air Pollution Study: Mortality among Residents of 90 Cities, *J. Toxicol. Environ. Health Part A* **2005**, *68*, 1071.

[8] S. J. Dutton, S. Vedal, R. Piedrahita, J. B. Milford, S. L. Miller, M. P. Hannigan, Source Apportionment Using Positive Matrix Factorization on Daily Measurements of Inorganic and Organic Speciated PM2.5, *Atmos. Environ.* **2010**, *44*, 2731.

[9] J.-M. Lim, J.-H. Lee, J.-H. Moon, Y.-S. Chung, K.-H. Kim, Source Apportionment of PM10 at a Small Industrial Area Using Positive Matrix Factorization, *Atmos. Res.* **2010**, *95*, 88.

[10] USEPA, EPA Positive Matrix Factorization (PMF) 3.0 Fundamentals & User Guide, Environmental Protection Agency Office of Research and Development, Washington, DC **2008**.

[11] L. Y. Alleman, L. Lamaison, E. Perdrix, A. Robache, J.-C. Galloo, PM10 Metal Concentrations and Source Identification Using Positive Matrix Factorization and Wind Sectoring in a French Industrial Zone, *Atmos. Res.* **2010**, *96*, 612.

[12] P. Paatero, P. K. Hopke, Discarding or Downweighting High-Noise Variables in Factor Analytic Models, *Anal. Chim. Acta* **2003**, *490*, 277.

[13] S. Vaccaro, E. Sobiecka, S. Contini, G. Locoro, G. Free, B. M. Gawlik, The Application of Positive Matrix Factorization in the Analysis, Characterisation and Detection of Contaminated Soils, *Chemosphere* **2007**, *69*, 1055.

[14] E. Kim, T. V. Larson, P. K. Hopke, C. Slaughter, L. E. Sheppard, C. Claiborn, Source Identification of PM2.5 in an Arid Northwest U.S. City by Positive Matrix Factorization, *Atmos. Res.* **2003**, *66*, 291.

[15] M. H. Sowlat, K. Naddafi, M. Yunesian, P. L. Jackson, A. Shahsavani, Source Apportionment of Total Suspended Particulates in an Arid Area in Southwestern Iran Using Positive Matrix Factorization, *Bull. Environ. Contam. Toxicol.* **2012**, *88*, 735.

[16] A. S. Goudie, N. J. Middleton, *Desert Dust in the Global System*, Springer, Heidelberg **2006**.

[17] N. J. Middleton, Dust Storms in the Middle East, *J. Arid Environ.* **1986**, *10*, 83.

[18] A. Shahsavani, K. Naddafi, N. Jafarzade Haghighifard, A. Mesdaghinia, M. Yunesian, R. Nabizadeh, M. Arahami, et al., The Evaluation of PM10, PM2.5, and PM1 Concentrations during the Middle Eastern Dust (MED) Events in Ahvaz, Iran, from April through September 2010, *J. Arid Environ.* **2012**, *77*, 72.

[19] A. Shahsavani, K. Naddafi, N. Jafarzade Haghighifard, A. Mesdaghinia, M. Yunesian, R. Nabizadeh, M. Arhami, et al., Characterization of Ionic Composition of TSP and PM10 during the Middle Eastern Dust (MED) Storms in Ahvaz, Iran, *Environ. Monit. Assess.* **2012**, *184 (11)*, 6683–6692.

[20] X. Yao, C. K. Chan, M. Fang, S. Cadle, T. Chan, P. Mulawa, K. He, et al., The Water-Soluble Ionic Composition of PM2.5 in Shanghai and Beijing, China, *Atmos. Environ.* **2002**, *36*, 4223.

[21] Y. Wang, G. Zhuang, A. Tang, W. Zhang, Y. Sun, Z. Wang, Z. An, The Evolution of Chemical Components of Aerosols at Five Monitoring Sites of China during Dust Storms, *Atmos. Environ.* **2007**, *41*, 1091.

[22] Z. Shen, J. Cao, R. Arimoto, Z. Han, R. Zhang, Y. Han, S. Liu, et al., Ionic Composition of TSP and PM2.5 during Dust Storms and Air Pollution Episodes at Xi'an, China, *Atmos. Environ.* **2009**, *43*, 2911.

[23] W. Zhang, G. Zhuang, J. Guo, D. Xu, W. Wang, D. Baumgardner, Z. Wu, et al., Sources of Aerosol as Determined from Elemental Composition and Size Distributions in Beijing, *Atmos. Res.* **2010**, *95*, 197.

[24] S.-J. Chen, L.-T. Hsieh, M.-J. Kao, W.-Y. Lin, K.-L. Huang, C.-C. Lin, Characteristics of Particles Sampled in Southern Taiwan during the Asian Dust Storm Periods in 2000 and 2001, *Atmos. Environ.* **2004**, *38*, 5925.

[25] M. T. Cheng, W. C. Chou, C. P. Chio, S. C. Hsu, Y. R. Su, P. H. Kuo, B. J. Tsuang, et al., Compositions and Source Apportionments of Atmospheric Aerosol during Asian Dust Storm and Local Pollution in Central Taiwan, *J. Atmos. Chem.* **2008**, *61*, 155.

[26] Y. Sun, G. Zhuang, Y. Wang, L. Han, J. Guo, M. Dan, W. Zhang, et al., The Air-Borne Particulate Pollution in Beijing – Concentration, Composition, Distribution and Sources, *Atmos. Environ.* **2004**, *38*, 5991.

[27] P. Paatero, U. Tapper, Analysis of Different Modes of Factor Analysis as Least Squares Fit Problems, *Chemom. Intell. Lab. Syst.* **1993**, *18*, 183.

[28] P. Paatero, Least Squares Formulation of Robust Non-Negative Factor Analysis, *Chemom. Intell. Lab. Syst.* **1997**, *37*, 23.

[29] P. Paatero, U. Tapper, Positive Matrix Factorization: A Non-Negative Factor Model with Optimal Utilization of Error Estimates of Data Values, *Environmetrics* **1994**, *5*, 111.

[30] S. Yatkin, A. Bayram, Source Apportionment of PM10 and PM2.5 Using Positive Matrix Factorization and Chemical Mass Balance in Izmir, Turkey, *Sci. Total Environ.* **2008**, *390*, 109.

[31] A. V. Polissar, P. K. Hopke, P. Paatero, W. C. Malm, J. F. Sisler, Atmospheric Aerosol over Alaska, 2. Elemental Composition and Sources, *J. Geophys. Res.* **1998**, *103*, 19045.

[32] L. L. Ashbaugh, W. C. Malm, W. Z. Sadeh, A Residence Time Probability Analysis of Sulfur Concentrations at Ground Canyon National Park, *Atmos. Environ.* **1985**, *19*, 1263.

[33] E. Kim, P. K. Hopke, E. S. Edgerton, Improving Source Identification of Atlanta Aerosol Using Temperature Resolved Carbon Fractions in Positive Matrix Factorization, *Atmos. Environ.* **2004**, *38*, 3349.

[34] A. A. Karanasiou, P. A. Siskos, K. Eleftheriadis, Assessment of Source Apportionment by Positive Matrix Factorization Analysis on Fine and Coarse Urban Aerosol Size Fractions, *Atmos. Environ.* **2009**, *43*, 3385.

[35] B. M. Kim, R. C. Henry, Application of SAFER Model to the Los Angeles PM10 Data, *Atmos. Environ.* **2000**, *34*, 1747.

[36] X. C. Huang, O. Ilhan, A. K. Namik, Emissions of Trace Elements from Motor Vehicles: Potential Marker Elements and Source Composition Profile, *Atmos. Environ.* **1994**, *28*, 1385.

[37] E. Lee, C. K. Chan, P. Paatero, Application of Positive Matrix Factorization in Source Apportionment of Particulate Pollutants in Hong Kong, *Atmos. Environ.* **1999**, *33*, 3201.

[38] B. Wehner, W. Birmili, T. Gnauk, A. Wiedensohler, Particle Number Size Distributions in a Street Canyon and Their Transformation into the Urban-Air Background: Measurements and a Simple Model Study, *Atmos. Environ.* **2000**, *36*, 2215.

[39] M. Santoso, P. K. Hopke, A. Hidayat, L. D. Dwiana, Sources Identification of the Atmospheric Aerosol at Urban and Suburban Sites in Indonesia by Positive Matrix Factorization, *Sci. Total Environ.* **2008**, *397*, 229.

[40] A. Arditsoglou, C. Samara, Levels of Total Suspended Particulate Matter and Major Trace Elements in Kosovo: A Source Identification and Apportionment Study, *Chemosphere* **2005**, *59*, 669.

[41] Y. Song, Y. Zhang, S. Xie, L. Zeng, M. Zheng, L. G. Salmon, M. Shao, et al., Source Apportionment of PM2.5 in Beijing by Positive Matrix Factorization, *Atmos. Environ.* **2006**, *40*, 1526.

[42] J. H. Seinfeld, S. N. Pandis, *Atmospheric Chemistry and Physics from Air Pollution to Climate Change*, Wiley, New York **1998**.

[43] D. E. Day, W. C. Malm, S. M. Kreidenweis, Seasonal Variations in Aerosol Composition and Acidity at Shenandoah and Great Smoky Mountain National Parks, *J. Air Waste Manage. Assoc.* **1997**, *47*, 411.

[44] M. Uberoi, F. Shadman, High-Temperature Removal of Cadmium Compounds Using Solid Sorbents, *Environ. Sci. Technol.* **1991**, *25*, 1285.

[45] P. Paatero, P. K. Hopke, X.-H. Song, Z. Ramadan, Understanding and Controlling Rotations in Factor Analytic Models, *Chemom. Intell. Lab. Syst.* **2002**, *60*, 253.